Reduction of Yb(III) to Yb(II) by two-color two-photon excitation

ARTICLE *in* THE JOURNAL OF PHYSICAL CHEMISTRY A · AUGUST 2013

Impact Factor: 2.69 · DOI: 10.1021/jp402194g · Source: PubMed

3 AUTHORS, INCLUDING:

Nobuaki Nakashima
Toyota Physical and Chemical Institute
214 PUBLICATIONS **4,175** CITATIONS
SEE PROFILE

Tomoyuki Yatsuhashi
Osaka City University
64 PUBLICATIONS **908** CITATIONS
SEE PROFILE

THE JOURNAL OF PHYSICAL CHEMISTRY A

Article

pubs.acs.org/JPCA

Reduction of Yb(III) to Yb(II) by Two-Color Two-Photon Excitation

Nobuaki Nakashima,*[,†] Ken-ichi Yamanaka,[‡] and Tomoyuki Yatsuhashi[§]

[†]Toyota Physical and Chemical Research Institute, Nagakute, Aichi 480-1192, Japan

[‡]Toyota Central R&D Laboratories., Inc., Nagakute, Aichi 480-1192, Japan

[§]Department of Chemistry, Graduate School of Science, Osaka City University, Sugimoto, Sumiyoshi, Osaka 558-8585, Japan

Supporting Information

ABSTRACT: Ytterbium 3+ ions in alcohol were found to be reduced to the corresponding 2+ ions upon laser irradiation with a stepwise two-color two-photon excitation. The infrared (975-nm) pulse with a duration of 4 ns pumps the ground state to the 4f excited state with the transition of $^2F_{5/2} \leftarrow {}^2F_{7/2}$, and the second photon (355-nm) generates the charge transfer (CT) state of Cl 3p to Yb 4f; the reduction then occurs. Laser energy and excitation wavelength dependencies well-explain the above mechanism. The product Yb^{2+} was detected by its absorption spectrum peak at 367 nm. The absorption spectrum of the intermediate in the two-photon chemistry was measured from the 4f excited state ($^2F_{5/2}$) to the CT state by nanosecond laser photolysis. The intermediate spectrum appears in the wavelengths shorter than 400 nm with the molar extinction coefficient on the order of (10^2 M^{-1} cm^{-1}) at 340 nm and can be explained in terms of the CT absorption shifted by IR photon energy. A UV nanosecond laser pulse (266 nm from a YAG laser with a duration of 6 ns) can generate the reactive CT state by one-photon absorption and leads to Yb^{2+} formation. The reaction yields for single-photon UV excitation and the second photon in the two-photon excitation are on the order of 0.1, suggesting that the reactive states are a common CT state.

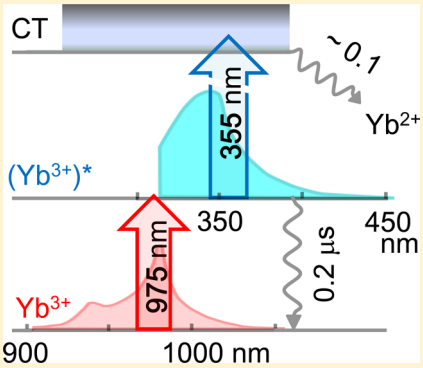

1. INTRODUCTION

Two-color two-photon photolysis techniques have been successfully applied to the discovery of new photochemical reactions in many organic systems.[1−3] Multiphoton chemistry with femtosecond pulses is also a recent research focus.[4,5] The two-photon chemistry of the redox reactions of lanthanide (Ln) ions was proposed in 1979,[6] and the reactions could be useful to purify these metals. Ln ions have 4f−4f absorptions with a narrow spectral width, and the electronic excited states show low reaction activities; in fact, no photoredox reaction has been reported from the lowest 4f emissive states. Some of the Ln ions have a charge transfer (CT) state in the deep UV region, and the CT state is photochemically active.[7] The photoreactive CT state can be generated by a single UV photon as well as by two sequentially absorbed photons via 4f excited states.

Two-photon reactions of Ln ions in solution with a single wavelength have been demonstrated for europium ($Eu^{3+} \rightarrow Eu^{2+}$) using nanosecond and picosecond laser pulses[8,9] and for samarium ($Sm^{3+} \rightarrow Sm^{2+}$) by femtosecond pulses.[10] These reactions of Ln ions could occur for actinide ions and are expected to be used for nuclear reprocessing through purification and separation. Despite the importance of these reactions, some of the detailed reaction mechanisms remain unclear. It is expected that the mechanisms will be finalized using a new Ln system of $Yb^{3+} \rightarrow Yb^{2+}$.

In the present study, $Yb^{3+} \rightarrow Yb^{2+}$ reactions by stepwise two-color two-photon and single-photon UV laser excitations were investigated. The following issues related to the two-photon chemistry are discussed.

(i) Does the $Yb^{3+} \rightarrow Yb^{2+}$ reaction occur by both stepwise two-color two-photon excitation and single-photon UV laser excitation? The key factors for the two-photon reaction of Ln will be discussed in association with the reduction potential.

(ii) Can no rapid relaxation processes between the 4f electronic states lead to a simple and clear two-photon mechanism? Yb^{3+} has a simple electronic structure; it contains only one excited state ($^2F_{5/2}$, 4f*) due to the change of the 4f electronic structure. On the other hand, the Eu^{3+} and Sm^{3+} systems have to be excited to one of the 4f excited states, and the relaxation processes between the 4f excited states were presumably included in the two-photon chemistry with a single wavelength.[8−10]

(iii) Can a conventional nanosecond laser photolysis method be applied for the Yb^{3+} system and the lifetime of the 4f* state be estimated? The transient absorption spectrum of CT ← 4f* has been measured here using the IR pulse (975 nm) as an excitation light source. We will discuss the nature of the CT ← 4f* transition, the reaction yield of the CT state, and internal conversion of the CT state versus geminate recombination (back reaction to the ground state from the CT state).

Received: March 4, 2013
Revised: August 6, 2013
Published: August 22, 2013

   dx.doi.org/10.1021/jp402194g | J. Phys. Chem. A 2013, 117, 8352−8359

(iv) Is the character of the CT state by the stepwise two-color two-photon excitation the same as that pumped by a UV single photon? The UV photochemistry of the $Yb^{3+} \rightarrow Yb^{2+}$ reaction should be induced by a 266-nm laser pulse. We examine this reaction here and discuss the reaction yields for the two-color two-photon and UV single photon processes.

(v) Does a nonresonant multiphoton absorption process occur? We irradiate a sample with laser pulses up to an intensity just below optical breakdown.

2. EXPERIMENTAL SECTION

Nanosecond laser pulses were delivered from a Q-switched Nd^{3+}:YAG laser (Continuum NY81-10; fundamental pulse of 900 mJ/pulse, 10 Hz) and an optical parametric oscillator (Continuum, Surelite OPO PLUS) pumped by the third harmonics of the fundamental pulse of the Nd^{3+}:YAG laser (355 nm). The spectral width was measured to be 4 nm in a wavelength range of 920−1000 nm with an Ocean Photonics USB4000. The pulse durations of the full width at half-maximum (fwhm) were 4 ns for the IR OPO and 5−7 ns for the 266 nm (the fourth harmonics of the YAG laser output) and the 355 nm. The IR pulse at 975−6 nm with 0.5−10 mJ/pulse was introduced first to a sample of alcohol solution. The UV pulse at 355 nm, 0.01−0.5 mJ/pulse, was introduced from the opposite direction, typically 14 ns later in order to avoid overlap with the IR pulse. The laser beams for the Yb^{2+} production experiments were focused typically at 0.5 mm in diameter for IR and 0.2 mm in diameter for UV pulses, by measuring the burn pattern of the beam imprint on a piece of photosensitive paper. For the absorption measurements of the UV at 355 nm, the UV beam diameter at the IR laser focus point was minimized to about 0.1 mm. The details are described in the text.

The averaged power of the laser pulse and the pulse energy were monitored with power meters (Gentec TPM310 and/or QE8SP-1-MT-USB). The transmittance of the optics and reflection of the cell surfaces were corrected for the pulse energies. The cell contained 0.04−0.16 cm^3 Yb^{3+} solution in a 2 (width) × 4 (depth) × 20 (height) mm quartz cell. The laser beams irradiated in the direction of the 2-mm width, and the products of the Yb^{2+} absorption spectra after the irradiation were measured in the direction of the 4-mm depth with a spectrophotometer (Shimadzu UV 3600). The Yb^{2+} concentrations after laser irradiation were estimated by the absorbance with a path length of 0.4 cm, using a molar extinction coefficient of 500 M^{-1} cm^{-1} at the peak of 367 nm.[11]

A conventional method of nanosecond laser photolysis[12] was applied to measuring a transient spectrum by 976-nm or 266-nm pulse irradiation under a single-shot operation mode for $YbCl_3$ in ethanol (EtOH) solution. A 150W Xe lamp (Hamamatsu Photonics, L2274) was used as the probe light, which was incident to the sample perpendicular to the excitation light path. The output of the monochromator was monitored using an avalanche photodiode (Hamamatsu Photonics, S5343) for 320−980 nm after amplification by a differential amplifier (NF Electronic Instruments, 5307). The emission was detected using an avalanche photodiode (Hamamatsu Photonics, G8931−20) which is sensitive for the range 940−1600 nm. The signal from the detector was recorded on a digital oscilloscope (Tektronix, TDS3032B). The total system was controlled with a personal computer via a general purpose interface bus (GPIB) interface. The measurement systems had a bandwidth of up to 10 MHz for transient absorption spectroscopy and up to 50 MHz for the emission spectroscopy. To measure the formation yield of Yb^{2+} by UV laser at 266 nm, a coaxial arrangement for excitation and monitoring beams was applied. The energy of the excitation light was 4−6.5 mJ/pulse for 266-nm excitation with a 0.2-cm-diameter spot size at the sample.

$YbCl_3 \cdot 6H_2O$ (99.998%; Aldrich), EtOH, methanol (MeOH; Nacalai, fluorescent grade), 18-crown-6-ether (18C6), and 15-crown-5-ether (15C5) (>97%; Tokyo Kasei) were used without further purification. For the two-photon experiments, a typical concentration of Yb^{3+} was 0.5−0.75 M with a three-time concentration of 15C5. The solution was degassed to avoid the oxidation of Yb^{2+} by dissolved oxygen, and 1 atm nitrogen was added to minimize bubble formation during the laser irradiation. Bubbles were probably formed by the evaporation of the alcohol due to heating by the IR laser irradiation. 15C5 had a molar extinction of 0.6 M^{-1} cm^{-1} at 266 nm.

3. RESULTS

3.1. Formation of Yb^{2+} by Nanosecond UV Laser Excitation. The Yb^{3+} to Yb^{2+} reaction by direct single-photon excitation to the charge transfer (CT) level (Cl 3p to $4f^{13}$ transition) was realized in this study. The CT levels show broad absorption spectra[13] and the 4f energy levels have line-like spectra.[14] The CT levels for $YbCl_3 \cdot 6H_2O$ in MeOH and EtOH have peaks at 210 and 240−245 nm[13] and had a tail that extended over 270 nm; therefore, the tail can be excited by the fourth harmonics of the Nd^{3+}:YAG laser (266 nm). Their molar extinction coefficients at 266 nm are 20 $M^{-1}cm^{-1}$ in MeOH and 50 $M^{-1}cm^{-1}$ in EtOH. The changes of absorption spectra due to Yb^{2+} ion formation were clearly observed by the laser irradiation as shown in Figure 1. The reactions can be explained in terms of Scheme 1 as discussed below.

New absorption appears in the UV region peaked at 367 nm in Figure 1a,b by 266-nm laser irradiation to a sample of Yb^{3+} in MeOH, accompanied by a slight decrease due to Yb^{3+} consumption in the absorbance in the near-infrared region in Figure 1c. The new absorption with a peak at 367 nm is safely assigned to Yb^{2+}, since the peak wavelength has been reported at 365 nm in EtOH,[11] 391 nm in tetrahydrofuran,[11] and 353 nm in the presence of 18C6 in MeOH in the present study. It is not surprising that the absorption spectrum of Yb^{2+} significantly depends on solvents. The absorption and emission spectra of Ln^{2+} (Ln = Eu or Sm) are known to be sensitive to solvents.[10,15] The emission of Yb^{2+} has been reported in crystals[16] and/or from a Yb^{2+} triethanolamine complex at a low temperature.[17] We attempted to detect emission of the 5d → 4f transition of Yb^{2+} in the visible region, but it was below the detection limit under degassed conditions at room temperature.

In the near IR region, the negative absorption was detected as shown in Figure 1c. The negative signal is attributed to the consumption of Yb^{3+} because its spectral shape is close to that of Yb^{3+}. The small value of −0.0035 in absorbance corresponds to the decrease in concentration on the order of 10^{-3} M on the basis of the molar extinction coefficient of 2.6 M^{-1} cm^{-1}. The Yb^{2+} absorption appeared as in Figure 1b, and the concentration of Yb^{2+} is estimated to be on the order of 10^{-3} M. The finding that the concentration of the Yb^{3+} consumption is on the same order as that of the Yb^{2+} product indicates that a one (Yb^{3+}) to one (Yb^{2+}) conversion occurs. The conversion efficiency from Yb^{3+} to Yb^{2+} of 0.05 is calculated as the ratio of the formed Yb^{2+} number to the total absorbed photon number. To determine the conversion efficiency for the single shot of

dx.doi.org/10.1021/jp402194g | J. Phys. Chem. A 2013, 117, 8352−8359

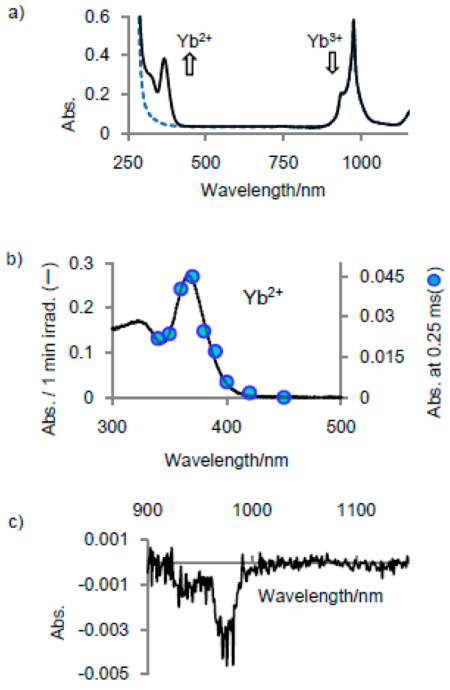

Figure 1. (a) Absorption spectra Yb^{3+} in MeOH in the presence of 1.8 M 15-crown-5 before and after UV (266 nm) laser irradiation. The solid line is observed after 600 shots of 4 mJ/pulse irradiation. The blue dotted line is the spectrum before irradiation. Difference spectra between before and after 266-nm laser irradiation in the ranges of (b) 300−500 and (c) 900−1150 nm are shown. The blue circles were obtained by one-shot experiments at 0.25 ms after a 266-nm laser pulse.

Scheme 1

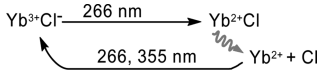

the laser pulse, a laser flash photolysis study was carried out using a 266-nm laser pulse. The Yb^{2+} absorption just after a laser pulse could be determined without lowering the Yb^{2+} concentrations with a diffusional escape from the irradiated region and/or a photoinduced oxidation of Yb^{2+} to Yb^{3+}. In fact, the Yb^{2+} absorption appears in <0.1 μs (for a detailed discussion see section 3.4) and remains constant for more than 2 ms. Therefore, the absorptions at 0.25 ms after excitation by the laser pulse (circles in Figure 1b) were plotted on the Yb^{2+} absorption spectrum with a maximum absorbance change of 0.045 at 370 nm. The conversion efficacy from Yb^{3+} to Yb^{2+} on the basis of the one-shot irradiation experiments was evaluated to be 0.2 ± 0.03. The above multishot experiments gave a smaller value, 0.05, which is attributable to a photoinduced oxidation of Yb^{2+} to Yb^{3+} as explained below.

3.2. Photoinduced Oxidation of Yb^{2+} to Yb^{3+}. The Yb^{2+} concentration reached a stationary state after 2.4×10^4 shots of 4 mJ/pulse at 266-nm (40 min) irradiation, indicating that a photoinduced oxidation reaction from Yb^{2+} to Yb^{3+} occurs and reached equilibrium as summarized in Scheme 1. Yb^{2+} has an absorption at the excitation wavelengths of 266 nm of the fourth harmonics of the Nd^{3+}:YAG laser and 355 nm of the third harmonics, and irradiation with both pulses would induce oxidation to yield Yb^{3+}. In fact, irradiation to Yb^{2+} by the pulses at 355 nm of 1.5 mJ per pulse at 10 Hz and 10 min caused a decrease in Yb^{2+} absorption from 0.35 to 0.2 at 367 nm, suggesting that the quantum yield of the photoinduced oxidation was a few tens of percent.

The difference spectrum for Yb^{3+} absorption around 975 nm appeared to be of differential type (Figure 2a). The spectral shape can be reconstructed by the combination of a consumption Yb^{3+} spectrum peaked at 975 nm and a 2-nm shifted production Yb^{3+} spectrum with a peak at 977 nm (see Figure 2b). The 2-nm peak shift would be explained if the new environments for the regenerated Yb^{3+} were different from the original ones. A decrease in the IR region longer than 1100 nm was seen and could have been due to the spectral shifts of vibrational overtone caused by the environmental changes.

3.3. Formation of Yb^{2+} by IR-UV Two-Color Two-Photon Excitation. *3.3.1. Molar Extinction Coefficient for the UV Pulse.* The Yb^{3+} alcoholic solution was irradiated by IR (at 975 or 976 nm) and UV (355 nm) pulses, where the IR pulse comes first; then, typically 14 ns later the UV pulse is introduced. It is essential to demonstrate that the UV pulse is actually absorbed by the sample after the IR pulse irradiation. Figure 3 shows the absorbance at 355 nm of the UV pulse

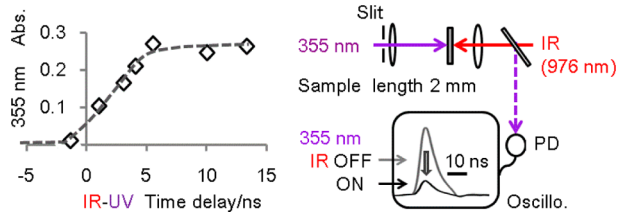

Figure 3. (a) Absorbance of a UV (355-nm) pulse vs time delay between IR (976-nm) and UV pulses represented by a diamond symbol (◊) with a dotted guide line. The IR pulse energy was 4 mJ/pulse for the Yb^{3+} EtOH 15C5 (1:3) solution and monitored with a UV pulse of 0.01 mJ. (b) Optical arrangements for the two-color two-photon reduction of Yb^{2+} to Yb^{3+}.

versus time delay between IR and UV pulses. The UV pulse absorption reaches a leveling-off of 0.27 at the 4 mJ IR pulse.

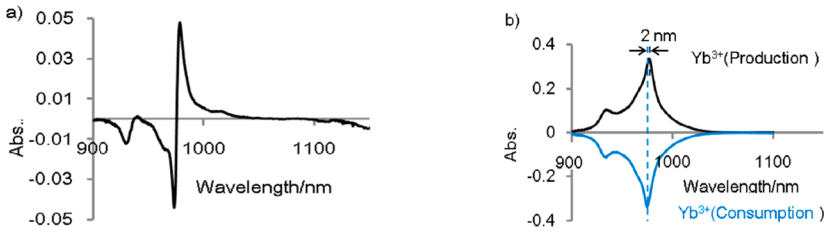

Figure 2. (a) Difference spectrum in the near IR region after 2.4×10^4 shots of 4 mJ/pulse at 266 nm. (b) The model spectra of Yb^{3+} consumption and production, where the peak wavelength of the product Yb^{3+} shifted by 2 nm from the original Yb^{3+}.

dx.doi.org/10.1021/jp402194g | J. Phys. Chem. A 2013, 117, 8352−8359

The IR pulse with a pulse width of 4 ns comes first, and then the UV pulse with a width of 7 ns arrives at the sample. Only a slight decay of the concentration of 4f* is expected in a 10-ns time range, because the lifetime of the excited state 4f* is 0.2 μs (in section 3.4). The absorbance of the UV pulse was linearly increased up to 0.7 at 10 mJ of the IR pulse, indicating that there was no signal saturation. The transmittance of the UV pulse was as low as 20% of the input in the presence of the IR pulse (10 mJ/pulse).

The molar extinction coefficient of 4f* to the CT state at 355 nm was estimated to be 4×10 M^{-1} cm^{-1} on the basis of the average concentration in the 4f* of 3.5×10^{-2} M at an IR pulse of 4 mJ with the path length of 0.2 cm.

3.3.2. Formation of Yb^{2+} with Two-Color Two-Photon Excitation. Yb^{2+} can be detected by the absorption spectrum peak around 367 nm in MeOH as shown in Figure 1. An increase in absorbance around 367 nm was observed by irradiation of the Yb^{3+} MeOH solution with IR (975-nm) and UV (355-nm) pulses with a delay time of 14 ns. The absorbance cannot reach higher than 0.2, corresponding to a Yb^{2+} concentration of 1×10^{-3} M. The reaction mechanism proposed in Scheme 1 clearly holds; the concentration of Yb^{2+} approaches a photochemical stationary state (Supporting Information). The Yb^{2+} concentration increases linearly with the number of laser shots or time as long as the concentration is low, while the photochemical back reaction becomes significant under high concentrations of Yb^{2+}.

It shoud be noted that no Yb^{2+} absorption was detected by a 975-nm IR pulse alone without a UV pulse or by the UV 355-nm pulse without the IR pulse. No multiphoton reduction was observed, though solvent breakdown was occasionally seen with a focused fluence of up to several J/cm^2 for each pulse.

3.3.3. Linear Relationship for Each Color for the Two-Photon Yb^{2+} Formation. The Yb^{2+} absorbance data versus input laser pulse energies are plotted in Figure 4. The Yb^{2+} concentrations were measured as the absorbances at 367 nm with a path length of 0.4 cm. Linear relationships were observed for both cases: absorbance data of Yb^{2+} for various UV (355-nm) laser energies at a fixed IR (975-nm) energy of 4 mJ and of Yb^{2+} for various IR laser energies at a fixed UV energy of 0.12 mJ. Absorbance data after irradiation of two laser pulses for 3-min irradiation (1800 shots) in Yb^{3+} MeOH 15C5 (1:3) solution were plotted versus the laser pulse energies. To avoid saturation effects, a value linearly extrapolated from those by short irradiation times was used for a laser energy range >0.2 mJ of a UV pulse.

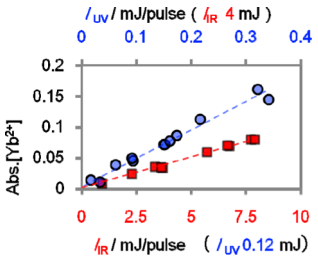

Figure 4. Yb^{2+} concentrations in absorbance at 367 nm after 3 min irradiation to Yb^{3+} solution are plotted vs the laser energies. The blue circles are Yb^{2+} concentrations with a fixed IR (975-nm) energy of 4 mJ. The red squares are Yb^{2+} concentrations with a fixed UV energy of 0.12 mJ.

The Yb^{2+} concentration produced by two-color two-photon excitation is expressed by eq 1, where laser pulses are absorbed on the basis of Lambert–Beer's law:

$$[Yb^{2+}] = \phi_{3\rightarrow 2} I_{UV}(1 - 10^{-\varepsilon_{CT}[Yb^{3+}]^* l}) \quad (1)$$

where

$$[Yb^{3+}]^* = I_{IR}(1 - 10^{-\varepsilon_g[Yb^{3+}]l}) \exp(-t/\tau_{obs}) \quad (2)$$

where $\phi_{3\rightarrow 2}$ is the conversion efficiency to Yb^{2+} from the CT state pumped by I_{UV} of the 4f* state, I_{UV} is the 355 nm laser pulse fluence, ε_{CT} is the molar extinction coefficient of the CT $\leftarrow$ 4f* transition, $[Yb^{3+}]^*$ is the concentration of Yb^{3+} in the 4f* state, which is shown by eq 2, I_{IR} is the IR laser pulse fluence at 975 nm, ε_g is the molar extinction coefficient of the 4f* $\leftarrow$ 4f transition, 2.6 M^{-1} cm^{-1} in MeOH at 975 nm, $[Yb^{3+}]$ is the concentration of Yb^{3+} in the ground state 4f, l is the cell length of 0.2 cm, and τ_{obs} is the lifetime of the 4f* state.

Maclaurin expansions are applied to eqs 1 and 2; $10^{-x} \approx 1 - 2.303x + ((2.303x)^2/2)) + ...$ Assuming $t = 0$, the x^2 and higher terms were approximate by zero because these terms become negligibly small when the x value is sufficiently small. Thus eq 3a is obtained from eqs 1 and 2.

$$[Yb^{2+}] \approx (2.303)^2 l^2 [Yb^{3+}] \phi_{3\rightarrow 2} \varepsilon_{CT} I_{UV} \varepsilon_g I_{IR} \quad (3a)$$

In order to compare eq 3a with the experimental results in Figure 4, this equation was rewritten as two equations, eqs 3b and 3c, in absorbance for the Yb^{2+} concentration and a unit of mJ for laser energy.

$$[Yb^{2+}] = 6.0 \phi_{3\rightarrow 2} I_{UV} \quad \text{at 4 mJ of } I_{IR} \quad (3b)$$

.

$$[Yb^{2+}] = 0.18 \phi_{3\rightarrow 2} I_{IR} \quad \text{at 0.12 mJ of } I_{UV} \quad (3c)$$

.

The linear relation is seen between Yb^{2+} concentrations and I_{UV} with a fixed energy of I_{IR} in Figure 4 and is predicted by eq 3b. It is true for Yb^{2+} and I_{IR} with a fixed energy of I_{UV}. The experimental results in Figure 4 are qualitatively well-explained in terms of eqs 3b and 3c. The reaction quantum yield $\phi_{3\rightarrow 2}$, the conversion efficiency to Yb^{2+} from the CT state, can be derived by comparison with the observed slopes. The observed slope of 0.47 in Figure 4 should be 6.0 $\phi_{3\rightarrow 2}$ in eq 3b, and then $\phi_{3\rightarrow 2}$ is calculated to be 0.08. The observed slope of 0.01 yields 0.06 of $\phi_{3\rightarrow 2}$ using eq 3c. These values were presumably underestimated. The x value in the Maclaurin expansions for eq 2 was 0.26 at the concentration of Yb^{3+}. This value causes 34% overestimation; therefore, the calculated $\phi_{3\rightarrow 2}$ values based on eqs 3a and 3b should be multiplied 1.34 times. In conclusion, we estimated that the real value of $\phi_{3\rightarrow 2}$ is 0.1 with −0.05 and +0.1 The uncertainties were estimated by such as a dilution factor in the solution volume before measurements of the Yb^{2+} spectrum and estimation procedures in the approximated equations in addition to laser energy fluctuations. It should be noted that we adopted an ε_{CT} value of 15 M^{-1} cm^{-1} instead of 40 M^{-1} cm^{-1} for eqs 3c. The absorption efficiency of I_{UV} in Figure 4 was 40% of that in Figure 3, presumably because we used a large size of 0.2 mm for the reduction experiments.

3.3.4. Excitation Wavelength Dependence of an IR Pulse on Yb^{2+} Formation. Figure 5 shows the relative Yb^{2+} concentrations (red circle) normalized with the absorption peak of the Yb^{3+} spectrum (– in units of %) with absorbance of

dx.doi.org/10.1021/jp402194g | J. Phys. Chem. A 2013, 117, 8352–8359

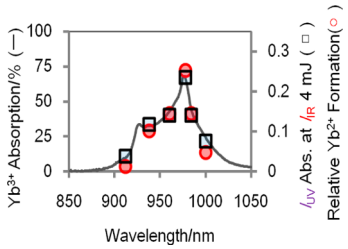

Figure 5. Wavelength dependencies for the relative Yb^{2+} formation (red circle) by UV and IR two-photon excitation and UV (355-nm) pulse absorption (□ in absorbance) in the presence of IR pulses at a delay of 14 ns. The solid line (−) is the absorption spectrum of Yb^{3+} in EtOH for a 0.4-cm pass length.

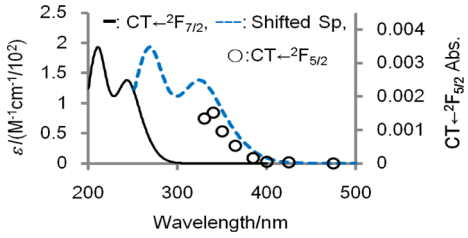

Figure 6. Transient absorption spectrum just after IR (976-nm) nanosecond laser pulse excitation is denoted by circles (○) and is assigned to the absorption from the lowest excited state ($^2F_{5/2}$) to the charge transfer (CT) state. The spectrum can also be read by both the vertical scales. The spectrum (blue dashed line) was shifted from the absorption (−) of Yb^{3+} in EtOH (10^{-2} M) by 10230 cm^{-1}.

the UV (355-nm) pulse (□) measured by the arragement shown in Figure 3 at several wavelengths of the IR pulses. The pulse energy of the IR was 4 mJ/pulse and that of the UV was 0.15 mJ/pulse with a delay of 14 ns. The relative Yb^{2+} concentrations (red circle) and the excited concentrations (□) can be put on the absorption spectrum of Yb^{3+}. These wavelength dependencies clearly support the stepwise two-photon chemistry of the $Yb^{3+} \rightarrow Yb^{2+}$ reduction. Small deviations of the relative Yb^{2+} concentrations were observed at both ends of the absorption spectrum at 925 and 1000 nm, but the reasons for these were not clear. The IR laser pulses with any wavelengths in the 900−1000 nm absorption band create the excited state of 4f* ($^2F_{5/2}$). An equilibillium state will be reached in less than a nanosecond between the sublevels in the 4f* state and surrounding solvents. The absorptions by the UV in Figure 5 represent the concentrations of Yb^{3+} in the 4f* state at several IR wavelengths. The relative Yb^{2+} concentrations by the UV 355 nm pulse are seen on the absorption spectrum, in other words, $\phi_{3\rightarrow2}$ is a constant. It is interesting to exsamine whether the reaction yield $\phi_{3\rightarrow2}$ depends on the UV wavelengths, as discussed in section 4.

3.4. Excited-State Absorption, Lifetime of $Yb^{3+}(^2F_{5/2})$ and Relaxation of the CT State. To the best of our knowledge, the absorption spectrum from the 4f electronically excited state was measured for the first time in the present study. The absorption spectrum from the 4f* to the CT state can be measured by a conventional nanosecond laser photolysis method, because the lifetime of the 4f* state was 0.2 μs, though the absorption signal was small due to the small absorption coefficient. A highly sensitive measurement system has been applied to the measurements of decay curves of transient absorption and emission after 976-nm light excitation.[12] The absorbance data just after excitation are plotted in Figure 6. The spectrum with a dotted blue line was constructed by shifting the absorption (the solid line) of Yb^{3+} by 10 230 cm^{-1} (the energy difference between $^2F_{5/2}$ and $^2F_{7/2}$). The solid line is the CT absorption spectrum, which has been explained in terms of the Cl 3p ← 4f transition.[13,18,19] The transient absorption spectrum, which is normalized to the molar extinction coefficient of the 40 M^{-1} cm^{-1} CT ← 4f* transition at 355 nm (section 3.3.1), is close to the dotted line. The results indicate that the transition moment from the 4f* state to the CT state is on the same order as that of the transition from the 4f to the CT state. The transition to the CT state is considered to be the transference of the electron from the ligand to the unfilled 4f shell ($4f^{14}Cl \leftarrow 4f^{13}Cl^-$). The transition moments from 4f and 4f* can be on the same order.

The excited-state absorption (ESA) of Ln ions has been discussed in up-conversion (UC) experiments; for example, the UC emission from Tm^{2+} around 17 000 cm^{-1} has been detected using two continuous wave (CW) light sources.[20] Tm^{2+} has thirteen 4f electrons in the ground state and is isoelectronic with Yb^{3+}. The dominant UC process would be an excitation to 4f* by the first light source and the second photon pumps to a 5d state (5d ← 4f excitation), but the spectra and the dynamics have not been reported, to our knowledge.

The time evolution of the 4f* state of $YbCl_3$ in EtOH (0.7 M for IR and 0.08 M for UV photolysis) was studied by the nanosecond laser photolysis after IR pulse (976-nm) and UV pulse (266-nm) excitations. The same decay time of 0.2 μs was observed for both the emission at 1.03 μm (by IR excitation) and the transient absorption at 340 nm; therefore, the absorption at 340 nm after IR excitation is safely assigned to the excited-state absorption.

The emission lifetime, τ_{obs}, of 0.2 μs in EtOH solution is consistent with the tendency of the Ln^{3+} emission lifetimes. Yb^{3+} complexes have been studied from the viewpoint of highly near-IR luminophores (in other words, longer lifetimes).[21] The longest lifetime τ_{obs} of 91 μs from a perdeuterated Yb^{3+} cryptate in CD_3OD has been reported.[22] The near-IR emission intensities of Ln^{3+} ions are generally weak with short lifetimes in water, MeOH, and EtOH. Radiationless transition via vibrational relaxation can be considered a dominant quenching process of the excited state of the Ln complexes:

$$\tau_{rad} = \frac{1}{k_r}, \quad \tau_{obs} = \frac{1}{k_r + k_{nr}} \tag{4}$$

where the symbols are the radiative rate constant (k_r) and nonradiative rate constant (k_{nr}) in the 4f*−4f transition of Yb^{3+}. The overtone of OH vibrations would largely contribute to the radiationless transitions as promoting and accepting modes. The emission lifetimes τ_{obs} of Nd^{3+} have been measured to be 0.032 μs in H_2O and 0.054 μs in MeOH.[23] The energy gap between the emission and ground levels in Yb^{3+} is 10 230 cm^{-1}, which is about twice that of Nd^{3+} ion (5400 cm^{-1}, for $^4F_{3/2}-{}^4F_{15/2}$).[14] The larger energy gap would provide the lower radiationless rate constants (k_{nr}). The observed lifetimes of Yb^{3+}, that is, 0.1 in H_2O, and 0.2 μs in MeOH and EtOH in this study, are reasonable on the basis of the above considerations. It is notable that the radiative lifetime τ_{rad} of the 4f* excited state of Yb^{3+} has been estimated to be 1.21−0.47 ms[21,24−26] and that of Nd^{3+} is 0.42 ms.[21,27]

The transient absorption signal after UV light (266-nm) excitation observed at 340 nm in the CT←4f* absorption

dx.doi.org/10.1021/jp402194g | J. Phys. Chem. A 2013, 117, 8352−8359

spectrum showed two components. These were the decay component with 0.2 μs and residual constant component. The former is assignable to the CT ← 4f* transition, since the decay time is the decay of 4f* of 0.2 μs. The latter constant component is assignable to Yb^{2+}. This residual component was not seen in the IR photolysis, because no Yb^{2+} was formed by IR pulses. The existence of the CT ← 4f* absorption after UV excitation indicates a rapid internal conversion from the CT state. The charge transfer will produce Yb^{2+}+$Cl^{\bullet}$ with a yield of $\phi_{3\rightarrow 2}$ of 0.2 ± 0.03, and the rest finally seems to relax to the 4f* state with a minor process of direct relaxation to the ground state ($\phi_{recom} \approx 0$) (see the Supporting Information).

4. DISCUSSION

For purposes of discussing the Yb^{3+} laser chemistry, the energy diagram for the excited-state dynamics and photochemistry is shown in Figure 7. Several issues raised in the Introduction are addressed as follows.

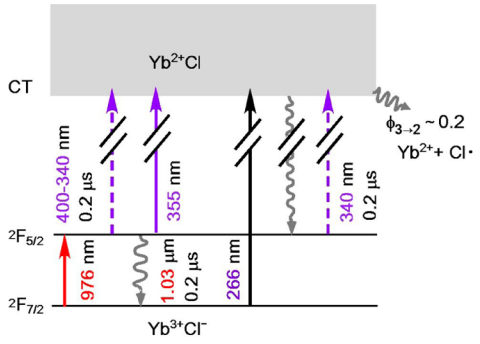

Figure 7. Energy diagram for the excited-state dynamics and photochemistry of Yb^{3+} in EtOH. The left part shows results after 976-nm pulse excitation and the right part those after 266-nm excitation.

(i) The $Yb^{3+}\rightarrow Yb^{2+}$ reactions have been found to be induced by single- and two-photon excitation in this study. We know now that three Ln ions (Ln^{3+}) are photochemically reduced to the corresponding Ln^{2+}. The three Ln elements are Eu,[8] Sm,[10] and Yb. One of their features in common is the low Ln^{3+}/Ln^{2+} reduction potentials: −0.35 (Eu), −1.15 (Yb), and −1.55 (Sm) in units of volts versus NHE (standard hydrogen electrode).[28] In those three elements, the CT levels are seen in the deep UV region.[13] The next elements with a low potential are Tm (−2.3), Nd (−2.6), and Dy (−2.6), ..., and attempts to induce their reactions might be made in a future study.

(ii) Yb^{3+} has a simple electronic structure: only one excited state due to the change of the 4f electronic structure (Figures 7). We do not need to consider rapid relaxation processes between the 4f* electronic states. A stepwise two-photon excitation was successfully applied because a reasonably long lifetime is expected for the lowest 4f* state; it is 0.2 μs. The Eu^{3+} and Sm^{3+} systems had to be excited to one of the 4f excited states, which are not emissive states with long lifetimes. Analyses of the two-photon chemistry might not be simple because of the lack of clear information regarding the lifetimes of the intermediate states.[9,10]

(iii) A conventional nanosecond laser photolysis method has been successfully applied to the Yb^{3+} system, because the 4f* has a relatively long lifetime of 0.2 μs in EtOH. We measured the spectrum of CT ← 4f* using an IR (976-nm) pulse as an excitation light source. The detected CT state from the 4f* would be the same as that observed from the ground state. The 4f* ← 4f transition is dipole forbidden; therefore, the molar extinction coefficient of the CT ← 4f* and the spectral shape could be compared with the coefficient of CT ← 4f and the shifted spectrum by the energy difference between the 4f* and 4f states, respectively. In fact the CT ← 4f* spectrum starts from a wavelength range of 340−400 nm, and the observed molar extinction coefficient of 40 M^{-1} cm^{-1} at 355 nm (section 3.3.1) for the CT ← 4f* transition can be compared with that of 65 M^{-1} cm^{-1} at 260 nm; that wavelength corresponds to the sum of 28 190 cm^{-1} (the third harmonics of the Nd^{3+}:YAG laser + the energy difference between the 4f* and 4f states of 10 230 cm^{-1}). The measured value of 40 M^{-1} cm^{-1} would contain several tens of percent uncertainty due to the lack of precise measurements of the focused beam size and intensity distributions in the spot, but the oscillator strengths of CT ← 4f and CT ← 4f* are on the same order.

It may be noted that there are differences between the excited state absorption of π electron organic hydrocarbons, such as benzene and the CT ← 4f* spectrum. The electronic absorption spectrum of excited-state benzene ($S_4 \leftarrow S_1$) was measured by one of the authors, and its spectral shape cannot be compared with the shifted spectrum at all; for example, the allowed $^1E_{2g}(S_4) \leftarrow {}^1B_{2u}(S_1)$ transition from the lowest excited singlet state (S_1) was observed, but the transition to the $^1E_{2g}$ state is not seen in the absorption spectrum from the ground state of $^1A_g(S_0)$.[29] The molar extinction coefficient is 4.2 × 10^4 M^{-1} cm^{-1} for the $S_4 \leftarrow S_1$ transition of benzene. The CT ← 4f* transition is allowed but is a few orders of magnitude smaller than that for benzene.

(iv) The CT state generated by the second photon excitation at 355 nm would be in the same as the CT state pumped by a UV single photon at 266 nm (37 600 cm^{-1}), though the two photon energy is 38 440 cm^{-1} or corresponding to a wavelength of 260 nm. Therefore, the same reaction yields would be expected for both one- and two-step processes. We summarized in Figure 7 the results of photoreaction of $Yb^{3+} \rightarrow Yb^{2+}$ with a stepwise two-color two-photon excitation and those of IR (976-nm) and UV (266-nm) laser flash photolysis. The reduction to Yb^{2+} occurs with the yield on the order of 0.1 for the second photon at 355 nm in the two-photon process and with the yield of 0.2 ± 0.03 for a single 266-nm photon excitation. We propose that the two values are in agreement because the evaluation of 0.1 for the photon at 355 nm includes some uncertainty (−0.05 and +0.1).

It is notable that wavelength dependency with UV light for reduction of the Eu^{3+} system has been reported,[30] in which the yields of Eu^{2+} formation were 0.42 at 222 nm and 0.35 at 248 nm for Eu^{3+} in methanol. This increase in the yield was caused by changing the excitation energy with a deference of 4800 cm^{-1}. The CT state with higher energy may give higher reduction yields for this Yb^{3+} system, but it is not clear at the present stage. To discuss precisely the UV wavelength dependency, the present experimental errors were too large.

We have successfully observed the CT ← 4f* absorption, determined the lifetime of the 4f* and observed the existence of internal conversion from the CT state as a dominant relaxation process from the CT state. We attempted to detect any signal of direct internal conversion to the ground state from the CT state; however, the present conclusion is that the geminate recombination after excitation to the CT state seems to relax to the lowest excited state of 4f* for this Yb^{3+} system.

dx.doi.org/10.1021/jp402194g | J. Phys. Chem. A 2013, 117, 8352−8359

(v) We should be careful whether nonresonant (355-nm) or resonant (976-nm) intense laser pulses induce the reaction. Multiphoton excitation of the 4f* ← 4f transition for Ln ions without chelation has been reported.[31] Yb^{2+} absorption was below our detection limit by irradiation with either of 355 or 976 nm laser pulses alone. The highest conversion efficiency to Yb^{2+} would be reached under the highest laser intensity for multiphoton reactions, if they occur. The feasibly highest laser intensities for these experiments would be the ones just below which cause solvent breakdown and/or surface damage of a quartz cell. No Yb^{2+} was observed even at the highest laser intensities (ca. 1×10^9 W/cm^2).

5. CONCLUSIONS

Yb^{3+} ions in alcohol were found to be reduced to the corresponding 2+ ions upon laser irradiation with a stepwise two-color excitation. The infrared (975 and 976-nm) pulse with a duration of 4 ns pumps the ground state to the 4f excited state with the transition of 4f* ← 4f and the second photon (355 nm) with a duration of 6 ns generates the charge transfer (CT) state of Cl 3p to Yb 4f; the reduction then occurs. The reaction mechanisms have been studied from various points of view. The energy dependencies on each color of UV and IR and the IR wavelengths successfully demonstrate the above mechanism. The product Yb^{2+} was detected by its absorption spectrum peak at 367 nm.

We measured the intermediate absorption spectrum with the molar extinction coefficient on the order of (10^2 M^{-1} cm^{-1}) in the two-photon chemistry from the 4f* excited state to the CT state by nanosecond laser photolysis. The intermediate absorption appears in the wavelengths shorter than 400 nm and can be explained in part in terms of the CT absorption shifted by the IR photon energy. A UV nanosecond laser pulse at 266 nm from a YAG laser can generate the reactive CT state by one-photon absorption and leads to Yb^{2+} formation. The reaction yields for the second photon excitation of the stepwise two-photon excitation and direct one-photon UV excitation were on the order of 0.1, suggesting that the reactive states are a common CT state.

One of the features in common for the photochemically active elements Eu, Yb, and Sm can be said to be low Ln^{3+}/Ln^{2+} reduction potentials. The above redox control in Ln ions could be used for purification and separation. The differences of the redox potentials in actinide ions between Ac^{n+} and Ac^{m+} ($m = n - 1$ and $n + 1$) are often smaller than that of 1.55 eV between Sm^{3+} and Sm^{2+}.[32] Therefore, actinide ions with 5f electrons are expected to show similar reactions, which may be useful for nuclear reprocessing.

■ ASSOCIATED CONTENT

Supporting Information

(1) Time evolution of difference spectra after two-color two-photon excitation with a delay time of 14 ns between the first IR pulse at 975 nm (at a fixed enegy of 4 mJ/pulse) and the second UV pulses at 355 nm at pulses of 0.07, 0.17, and 0.24 mJ with 10 Hz for $YbCl_3$ in MeOH solution. (2) Time dependencies by nanosecond laser photolysis after (a) IR (976-nm) and (b) UV (266-nm) pulse excitations. The concentrations of $YbCl_3$ in EtOH are 0.7 M for IR and 0.08 M for UV photolysis. The emission at 1.03 μm (the red line) and the transient absorption at 340 nm (the black line) have the same decay time of 0.2 μs. The transient absorption at 340 nm for the UV photolysis has a decay component due to the CT ← 4f* and the residual constant due to Yb^{2+}. The dotted line is the average of absorbance between 1 and 3 μs. This material is available free of charge via the Internet at http://pubs.acs.org.

■ AUTHOR INFORMATION

Corresponding Author

*E-mail: nakashima@toyotariken.jp.

Notes

The authors declare no competing financial interest.

■ ACKNOWLEDGMENTS

N.N. and T.Y. thank Ms. Ayaka Itoh and Mr. Takashi Yasuzuka for the initial trial of these reactions. This work was financially supported in part by a Grant-in-Aid (No. 23550030) from the Ministry of Education, Culture, Sports, Science, and Technology Japan to N.N.

■ REFERENCES

(1) Miranda, M. A.; Pérez-Prieto, J.; Font-Sanchis, E.; Scaiano, J. C. One- vs Two-Photon Processes in the Photochemistry of 1, *n*-Dihaloalkanes. *Acc. Chem. Res.* **2001**, *34*, 717−726.

(2) Goez, M.; Zubarev, V.; Eckert, G. Photoionization via Absorption/Electron Transfer/Absorption Studied by Two-Pulse Two-Color Laser Flash Photolysis. *J. Am. Chem. Soc.* **1998**, *120*, 5347−5348.

(3) Hara, M.; Samori, S.; Cai, X.; Fujitsuka, M.; Majima, T. Importance of Properties of the Lowest and Higher Singlet Excited States on the Resonant Two-Photon Ionization of Stilbene and Substituted Stilbenes Using Two-Color Two-Lasers. *J. Phys. Chem. A* **2005**, *109*, 9831−9835.

(4) Yatsuhashi, T.; Nakahagi, Y.; Okamoto, H.; Nakashima, N. Linear Response of Multiphoton Reaction: Three-Photon Cycloreversion of Anthracene Biplanemer in Solution by Intense Femtosecond Laser Pulses. *J. Phys. Chem. A* **2010**, *114*, 10475−10480.

(5) Mori, K.; Ishibashi, Y.; Matsuda, H.; Ito, S.; Nagasawa, Y.; Nakagawa, H.; Uchida, K.; Yokojima, S.; Nakamura, S.; Irie, M.; et al. H. One-Color Reversible Control of Photochromic Reactions in a Diarylethene Derivative: Three-Photon Cyclization and Two-Photon Cycloreversion by a Near-Infrared Femtosecond Laser Pulse at 1.28 μm. *J. Am. Chem. Soc.* **2011**, *133*, 2621−2625.

(6) Donohue, T. Laser Purification of the Rare Earths. *Opt. Eng.* **1979**, *18*, 181−186.

(7) Donohue, T. Photochemical Separation of Elements in Solution. In *Chemical and Biological Applications of Lasers*; Moore, C. B., Ed.; Academic Press: New York, 1980; Vol. *5*, pp 239−273.

(8) Kusaba, M.; Nakashima, N.; Izawa, Y.; Yamanaka, C.; Kawamura, K. Two-Photon Reduction of Eu^{3+} to Eu^{2+} via the f′←f Transitions in Methanol. *Chem. Phys. Lett.* **1994**, *221*, 407−411.

(9) Nakashima, N.; Nakamura, S.; Sakabe, S.; Schillinger, H.; Hamanaka, Y.; Yamanaka, C.; Kusaba, K.; Ishihara, N.; Izawa, Y. Multiphoton Reduction of Eu^{3+} to Eu^{2+} in Methanol using Intense, Short Pulses from a Ti:sapphire Laser. *J. Phys. Chem.* **1999**, *103*, 3910−3916.

(10) Nishida, D.; Yamade, E.; Kusaba, M.; Yatsuhashi, T.; Nakashima, N. Reduction of Sm^{3+} to Sm^{2+} by an Intense Femtosecond Laser Pulse in Solution. *J. Phys. Chem. A* **2010**, *114*, 5648−5654.

(11) Kamenskaya, A. N. The Lower Oxidation State of the Lanthanides in Solution. *Russ. J. Inorg. Chem.* **1984**, *29*, 251−258.

(12) Yamanaka, K.; Okada, T.; Goto, Y.; Tani, T.; Inagaki, S. Dynamics in the Excited Electronic State of Periodic Mesoporous Biphenylylene-Silica Studied by Time-Resolved Diffuse Reflectance and Fluorescence Spectroscopy. *Phys. Chem. Chem. Phys.* **2010**, *12*, 11688−11696.

(13) Keller, B.; Bukietyńska, K.; Jeżowska-Trzebiatowska, B. The *f-d* and Charge Transfer Transitions in the Absorption Spectra of Alcohol Solvates of Lanthanide Chlorides. *Bull. Acad. Pol. Sci. Ser. Sci. Chim.* **1976**, *24*, 763.

(14) Carnall, W. T. The Absorption and Fluorescence Spectra of Rare Earth Ions in Solution. In *Handbook on the Physics and Chemistry of Rare Earths*; Gschneidner, K. A., Jr., Eyring, L., Eds.; North Holland Publ. Co.: Amsterdam, 1979; Vol. 3, Chapter 24, pp 172−208.
(15) Jiang, J.; Higashiyama, N.; Machida, K.; Adachi, G. The Luminescence Properties of Divalent Europium Compexes of Crown Ethers and Crystals. *Coord. Chem. Rev.* **1998**, *170*, 1−29.
(16) Lizzo, L.; Meijerink, A.; Dirksen, G. J.; Blasse, G. Luminescence of Divalent Ytterbium in Magnesium Fluoride Crystals. *J. Lumin.* **1995**, *63*, 233−234.
(17) Starynowicz, P.; Gatner, K. An Ytterbium(II) Complex with Triethanolamine. *Z. Anorg. Allg. Chem.* **2003**, *629*, 722−726.
(18) Nakazawa, E.; Shiga, F. Lowest 4f-to-5d and Charge-Transfer Transitions of Rare-Earth Ions in $LaPO_4$ and Related Host-Lattices. *Jpn. J. Appl. Phys.* **2003**, *42*, 1642−1647.
(19) Krupa, J. C. High-Energy Optical Absorption in *f*-Compounds. *J. Solid State Chem.* **2005**, *178*, 483−488.
(20) Beurer, E.; Grimm, J.; Gerner, P.; Güdel, H. U. Absorption, Light Emission, and Upconversion Properties of Tm^{2+}-Doped $CsCaI_3$ and $RbCaI_3$. *Inorg. Chem.* **2006**, *45*, 9901−9906.
(21) Comby, S.; Bünzli, J.-C. G. Lanthanide Near-Infrared Luminescence in Molecular Probes and Devices. In *Handbook on the Physics and Chemistry of Rare Earths*; Gschneidner, K. R., Jr., Bünzli, J.-C. G., Pecharsky, V. K., Eds.; Elsevier Science B. V.: Amsterdam, 2007; Vol. 37, Chapter 235, pp 217−470.
(22) Doffek, C.; Alzakhem, N.; Molon, M.; Seitz, M. Rigid, Perdeuterated Lanthanoid Cryptates: Extraordinarily Bright Near-IR Luminophores. *Inorg. Chem.* **2012**, *51*, 4539−4545.
(23) Kimura, T.; Nagaishi, R.; Kato, Y. Yoshida, Luminescence Study on Solvation of Americium(III), Curium(III) and Several Lanthanide-(III) Ions in Nonaqueous and Binary Mixed Solvents. Z. *Radiochim. Acta.* **2001**, *89*, 125−130.
(24) Werts, M. H. V.; Jukes, R. T. F. Verhoeven, The Emission Spectrum and the Radiative Lifetime of Eu^{3+} in Luminescent Lanthanide Complexes. J. W. *Phys. Chem. Chem. Phys.* **2002**, *4*, 1542−1548.
(25) Shavaleev, N. M.; Scopelliti, R.; Gumy, F.; Bünzli, J.-C. G. Surprisingly Bright Near-Infrared Luminescence and Short Radiative Lifetimes of Ytterbium in Hetero-Binuclear Yb-Na Chelates. *Inorg. Chem.* **2009**, *48*, 7937−7946.
(26) Kishimoto, S.; Nakagawa, T.; Kawai, T.; Hasegawa, Y. Enhanced Near-Infrared Luminescence of Yb(III) Complexes with Phosphine Oxide and Hexafluoroacetylacetonate Ligands. *Bull. Chem. Soc. Jpn.* **2011**, *84*, 148−154.
(27) Bünzli, J.-C. G.; Piguet, C. Taking Advantage of Luminescent Lanthanide Ions. *Chem. Soc. Rev.* **2005**, *34*, 1048−1077.
(28) Morss, L. R. Thermochemical Properties of Yttrium, Lanthanum, and the Lanthanide Elements and Ions. *Chem. Rev.* **1976**, *76*, 827−841.
(29) Nakashima, N.; Sumitani, M.; Ohmine, I.; Yoshihara, K. Nanosecond Laser Photolysis of Benzene Monomer and Excimer. *J. Chem. Phys.* **1980**, *72*, 2226−2230.
(30) Kusaba, M.; Nakashima, N.; Izawa, Y.; Kawamura, W.; Yamanaka, C. Higher Yield of Photoreduction of Eu^{3+} to Eu^{2+} with Shorter Wavelength Irradiation. *Chem. Phys. Lett.* **1992**, *197*, 136−140.
(31) Lakowicz, J. R.; Piszczek, G.; Maliwal, B. P.; Gryczynski, I. Multiphoton Excitation of Lanthanides. *ChemPhysChem* **2001**, *2*, 247−252.
(32) Kihara, S.; Yoshida, Z.; Aoyagi, H.; Maeda, K.; Shirai, O.; Kitatsuji, Y.; Yoshida, Y. A Critical Evaluation of the Redox Properties of Uranium, Neptunium and Plutonium Ions in Acidic Aqueous Solutions. *Pure Appl. Chem.* **1999**, *71*, 1771−1807.